Spectroscopic Investigation of the Structures of Dialkyl Tartrates and Their Cyclodextrin Complexes

Peng Zhang and Prasad L. Polavarapu*

Department of Chemistry, Vanderbilt University, Nashville, Tennessee 37235

Received: September 7, 2006; In Final Form: November 20, 2006

Structures of three dialkyl tartrates, namely, dimethyl tartrate, diethyl tartrate, and diisopropyl tartrate, in CCl_4, dimethyl sulfoxide (DMSO)/DMSO-d_6, and H_2O/D_2O solvents have been investigated using vibrational absorption (VA), vibrational circular dichroism (VCD), and optical rotatory dispersion (ORD). VA, VCD, and ORD spectra are found to be dependent on the solvent used. Density functional theory (DFT) calculations are used to interpret the experimental data in CCl_4 and DMSO. The *trans*-COOR conformer with hydrogen bonding between the OH group and the C═O group attached to the same chiral carbon is dominant for dialkyl tartrates both in vacuum and in CCl_4. The experimental VA, VCD, and ORD data of dialkyl-D-tartrates in CCl_4 correlated well with those predicted for dimethyl-(*S*,*S*)-tartrate molecule as both isolated and solvated in CCl_4. In DMSO solvent, dialkyl tartrate molecules favor formation of intermolecular hydrogen bonding with DMSO molecules. Clusters of dimethyl-(*S*,*S*)-tartrate, with one molecule of dimethyl-(*S*,*S*)-tartrate hydrogen bonded to two DMSO molecules, are used for the DFT calculations. A *trans*-COOR cluster and a *trans*-H cluster are needed to obtain a reasonable agreement between the predicted and experimental data of dimethyl tartrate in DMSO solvent. VA, VCD, and optical rotations are also measured for dialkyl tartrate−cyclodextrin complexes. It is noted that these properties are barely affected by complexation of dialkyl tartrates with cyclodextrins, indicating weak interaction between tartrates and cyclodextrin. Binding constants of α-CD and *β*-CD with diethyl L-tartrate in both H_2O and DMSO have been determined using isothermal titration calorimetry technique. The smaller binding constants (less than 100) confirmed the weak interaction between tartrates and cyclodextrin in the solution state.

Introduction

Tartaric acid and its derivatives play an important role in organic and pharmaceutical chemistry.[1] Dialkyl tartrates are a category of tartaric acid derivatives which have wide applications in both academic laboratories and chemical industries. They can be used as good catalysts for asymmetric synthesis, and they are also chiral intermediates for several pharmaceuticals and agrochemicals.[2] Several different conformations are possible for dialkyl tartrates, and the interaction with solvent may alter the predominant conformations. Thus, it is important to know the dominant conformations of dialkyl tartrates in different solvents.

The utility of vibrational circular dichroism (VCD) for structural elucidation of chiral molecules is facilitated by two advances: (a) improvements in VCD instrumentation have made it possible to obtain the VCD spectra with enhanced signal-to-noise ratio and (b) development of reliable quantum mechanical theory[3] and its applications using density functional theory (DFT)[4] and quantum mechanical software[5] facilitates interpretation of the experimental data. VCD spectroscopy has been successfully used[6] for determining the structures of numerous chiral molecules in the solution phase. Recently VCD spectroscopy was also used to study host−guest interactions in cyclodextrin−guest complexes.[7]

Polarimetry is an age-old technique that has experienced a renaissance in the past few years, following the first prediction[8] of specific rotation using quantum mechanical methods. Recent implementation of DFT for predicting specific rotation has led to reliable predictions of specific rotation.[9] The specific rotations measured in the gas phase[10] are ideal for comparison with predictions on isolated molecules; however, such measurements require special instrumentation and are not routine. Because the condensed-phase experimental specific rotations (often reported for neat liquids or in some convenient solvent at some convenient concentration) can be influenced by solute−solute interactions, a quantitative comparison of predicted specific rotations for isolated molecules with condensed-phase experimental specific rotations may not be appropriate. To eliminate the influence of solute−solute interactions we advocated the measurement of intrinsic rotation (specific rotation in the limit of zero concentration).[11] Comparison of experimental intrinsic rotation with predicted specific rotation at a given wavelength for a given conformation is one approach to study the conformations of chiral molecules in solutions. Instead of investigating the rotation at one wavelength, optical rotation as a function of wavelength or optical rotatory dispersion (ORD) provides[12] a more reliable approach for the conformational analysis of chiral molecules.

Dialkyl tartrates have been studied by VA and VCD techniques before. Using VCD associated with the O−H stretching vibrations of dimethyl-L-tartrate in CCl_4 solution and its temperature dependence, Keiderling et al.[13] noted very little conformational mobility for this molecule in dilute CCl_4 solution. They also measured VCD associated with the C═O stretching vibrations in CCl_4. VCD spectra of dimethyl tartrate, diethyl tartrate, and diisopropyl tartrate were also measured[14] in the 1600−900 cm^{-1} region in different solvents (CCl_4, DMSO, and CS_2) and different concentrations. It was found

10.1021/jp065847h CCC: $37.00
Published on Web 01/05/2007

that VCD associated with the C−O stretching vibrations, at about 1140 and 1090 cm^{-1}, is similar for all molecules in all three solvents. However, in the C═O stretching region, absorption spectra showed[14] differences in CCl_4 and DMSO solvents. Absorption spectra in the C═O stretching region (1850−1600 cm^{-1}) indicated[14] two absorption bands in DMSO as opposed to one in CCl_4. Intermolecular hydrogen bonding with DMSO was thought to be responsible for this difference, but there was no further investigation of this issue.

In this article we report further investigations of VA and VCD spectra in the mid-infrared region in three different solvents (CCl_4, DMSO-d_6, and D_2O) for three dialkyl (namely, dimethyl, diethyl, and diisopropyl) tartrates. DMSO-d_6 and D_2O are used instead of DMSO and H_2O to avoid solvent absorption interference in the mid-infrared region. We also measured the intrinsic rotations and ORD spectra of dimethyl-D-tartrate in different solvents (CCl_4, DMSO, and H_2O). The DFT calculations for dimethyl-(*S*,*S*)-tartrate have been performed in the isolated state and in CCl_4 and DMSO solvents to study the solvent-dependent conformational changes of this molecule. Furthermore, dialkyl tartrate−cyclodextrin complexes have been prepared and their binding constants measured for the first time. VA and VCD spectra in the mid-infrared region and intrinsic rotations of these complexes have been measured to investigate the host−guest interactions in these complexes.

Experimental Section

Dimethyl-D-tartrate, dimethyl-L-tartrate, diethyl-D-tartrate, diethyl-L-tartrate, diisopropyl-D-tartrate, and diisopropyl-L-tartrate were all purchased from Aldrich Chemicals; α- and β-cyclodextrins were purchased from Sigma Chemicals.

VA and VCD Measurements. The VA and VCD spectra were recorded on a commercial Fourier transform VCD spectrometer, Chiralir (Bomem-BioTools, Canada), modified[15] to include double-polarization modulation. The transmission properties of the optical filter used in the instrument and BaF_2 substrates used for the liquid cell restrict the range of measurements to 2000−900 cm^{-1}. The VCD spectra were recorded at 4 cm^{-1} resolution. In CCl_4 solvent, spectra were measured for saturated solutions of dimethyl-D-tartrate and dimethyl-L-tartrate using a path length of 635 μm and data collection time of 1 h, for diethyl-D-tartrate and diethyl-L-tartrate at 0.020 M using a path length of 275 μm and 3 h data collection time, and for diisopropyl-D-tartrate and diisopropyl-L-tartrate at 0.017 M using a path length of 365 μm and 3 h data collection time. A variable path length cell with BaF_2 windows was used for the measurements. In DMSO-d_6 solvent spectra were also measured for both enantiomers of dimethyl tartrate (0.046 M), diethyl tartrate (0.04 M), and diisopropyl tartrate (0.035 M) with a data collection time of 3 h for each enantiomer. Spectra were also measured for β-CD complexes of diethyl-D-tartrate, diethyl-L-tartrate, diisopropyl-D-tartrate, and diisopropyl-L-tartrate at concentrations of 0.040 M in DMSO-d_6 with a data collection time of 3 h. For these measurements the samples were held in a demountable path length cell (200 μm) with BaF_2 windows. In D_2O solvent, spectra were measured for dimethyl-D-tartrate, diethyl-D-tartrate, and α-CD complex of diethyl-L-tartrate at concentrations of 0.048, 0.041, and 0.044 M, respectively, in a demountable path length cell (100 μm) with BaF_2 windows and a 3 h data collection time. In the presented VA spectra, the solvent absorption was subtracted out. For VCD spectra of dialkyl tartrates in CCl_4 and DMSO-d_6, the presented VCD spectra of the D-enantiomers were obtained by subtracting the VCD of L-enantiomers from their corresponding VCD of the D-enantiomers and then multiplying by 0.5.

Intrinsic Rotation Measurements. An Autopol IV polarimeter with a resolution of 0.001° (reproducibility of 0.002°) and analytical balances with accuracy of 0.00001 g were used to measure the optical rotations at 589 nm. Each time the solution was transferred to a 0.5 or 1.0 dm cell, and optical rotation was measured three different times to check for consistency. The averages of these measurements were used to calculate specific rotation. This procedure ensured that no unusual data scatter was present in the measurements. Optical rotations of dimethyl-D-tartrate at 589 nm were measured in the concentration ranges of 0.0028−0.0010 M in CCl_4, 0.0570−0.013 M in DMSO, and 0.0590−0.0037 M in H_2O. Optical rotations of diethyl-D-tartrate, diethyl-L-tartrate, diisopropyl-D-tartrate, diisopropyl-L-tartrate, α-CD, and β-CD were also measured in H_2O at 589 nm in the concentration ranges of 0.0439−0.0027, 0.0614−0.0038, 0.0521−0.0016, 0.0408−0.0026, 0.0083−0.0003, and 0.0077−0.0002 M, respectively. Optical rotations of the α-CD complex of diethyl-L-tartrate were measured in H_2O at 589 nm in the concentration range of 0.0031−0.0001 M. For the β-CD complexes of diethyl-L-tartrate, diethyl-D-tartrate, diisopropyl-L-tartrate, and diisopropyl-D-tartrate optical rotations were also measured in H_2O at 589 nm in the concentration ranges of 0.0058−0.0002, 0.0058−0.0002, 0.0031−0.00008, and 0.0031−0.00008 M, respectively. For dimethyl-D-tartrate in DMSO, optical rotations were also measured at 365 nm in the concentration range of 0.027−0.008 M. For the optical rotation measurements of the α-CD, β-CD, and β-CD complexes of diethyl-L-tartrate and diethyl-D-tartrate, a 0.5 dm cell was used. In all other cases, a 1.0 dm cell was used. The optical rotation versus concentration data are provided in the Supporting Information. The intrinsic rotation ($[\alpha]_{c=0}$ or $\{\alpha\}$) was determined by extrapolating the observed rotations to zero concentration.

Optical Rotatory Dispersion (ORD) Measurements. Optical rotations of dimethyl-D-tartrate were also measured at 0.0014 M in CCl_4, at 0.0064 M in DMSO, and at 0.0064 M in H_2O at wavelengths of 633, 589, 546, 436, 405, and 365 nm to obtain the ORD spectra.

Preparation of Dialkyl Tartrate−Cyclodextrin Complexes. These complexes were prepared using the coprecipation method,[16] as described here for diethyl-D-tartrate-β-CD complex as an example. The mixture of β-CD (1 mmol) and diethyl-D-tartrate (10 mmol) was dissolved in hot H_2O (5 mL) at 90 °C. Then the solution was allowed to cool slowly, and crystals were obtained after filtration. The α-CD complex of diethyl-L-tartrate and β-CD complexes of diethyl-D-tartrate, diethyl-L-tartrate, diisopropyl-D-tartrate, and diisopropyl-L-tartrate were prepared using the same procedure. All complexes were characterized by ^1H NMR. The NMR data are provided in the Supporting Information.

Determination of Binding Constants of Dialkyl Tartrate−Cyclodextrin Complexes. The binding constants of diethyl-L-tartrate complexes of α-CD and β-CD were determined in both H_2O and DMSO solvents by isothermal titration calorimetry (ITC).[17] An isothermal calorimeter (Microcal Inc., MA) was used for all microcalorimetric experiments. For these experiments in H_2O 20 injections of 5 μL of diethyl-L-tartrate in H_2O (100 mM) were added at an interval of 5 min into α-CD or β-CD solution in H_2O (2 mM) in the reaction cell (cell volume = 1.4 mL) while stirring at 300 rpm at 298 K. The duration time of each injection is 20 s. For microcalorimetric experiments in DMSO, 20 injections of 10 μL of diethyl-L-tartrate in DMSO were added at an interval of 5 min into α-CD or β-CD solution in DMSO (20 mM) in the cell with a stirring speed of 550 rpm

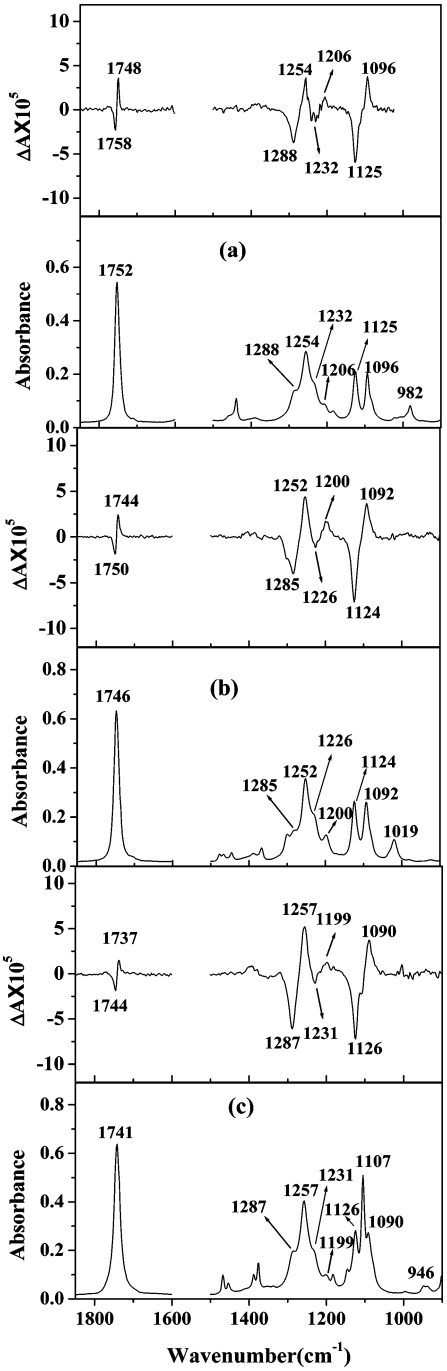

Figure 1. Vibrational absorption (bottom) and VCD (top) spectra in CCl_4 solutions: (a) dimethyl-D-tartrate (saturated solution), (b) diethyl-D-tartrate (0.020 M), and (c) diisopropyl-D-tartrate (0.017 M).

at 298 K. The concentration of diethyl-L-tartrate was 150 mM for titration with β-CD and 450 mM for titration with α-CD. For each injection the duration time was 7.1 s. The data for identical injections of diethyl-L-tartrate solution into the pure solvent were subtracted from the data for titration of α-CD/β-CD with diethyl-L-tartrate to produce the final binding curve. The ORIGIN software (Microcal) used for the calculation of K, ΔH, and ΔS from the titration curve gave the relevant standard deviations based on the scatter of the data points in a single titration curve.

DFT Calculations. The geometry optimization, vibrational frequencies, absorption, VCD intensities, and specific rotation calculations for isolated dimethyl-(*S*,*S*)-tartrate were obtained using the Gaussian 98 or 03 program.[5] For isolated molecule,

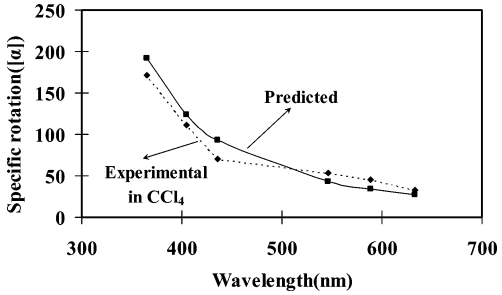

Figure 2. Comparison of experimental specific rotations of dimethyl-D-tartrate in CCl_4 and predicted specific rotations for isolated dimethyl-(*S*,*S*)-tartrate as a function of wavelength. The predicted specific rotations were obtained as population-weighted data from the two lowest energy conformers of isolated dimethyl-(*S*,*S*)-tartrate, namely, *trans*-$COOCH_3$-1 and *trans*-$COOCH_3$-2, at the B3LYP/aug-cc-pVDZ level.

the calculations used the B3LYP functional[18] and both 6-31G* and aug-cc-pVDZ basis sets.[19] The CCl_4 solvent influence was investigated with a polarizable continuum model (PCM) at the B3LYP/6-31G* level. The DMSO solvent influence was investigated using clusters of dimethyl-(*S*,*S*)-tartrate-$(DMSO)_2$ at the B3LYP/6-31G* level. Some of these clusters were also investigated at the B3LYP/aug-cc-pVDZ level. The theoretical absorption and VCD spectra were simulated with Lorentzian band shapes and 5 cm^{-1} full width at half-height. Since the predicted band positions with the 6-31G* basis set are higher than the experimental values, the predicted frequencies have been scaled[20] with 0.96.

Results and Discussion

(1) Dialkyl Tartrates in CCl_4. Because of the interference from CCl_4 absorption, VCD spectra of dialkyl tartrates can only be obtained in the regions of 2000−1600 and 1500−900 cm^{-1} in CCl_4. The vibrational absorption and VCD spectra of dimethyl-D-tartrate, diethyl-D-tartrate, and diisopropyl-D-tartrate, measured in CCl_4 solvent are shown in Figure 1. The absorption and VCD spectra of dimethyl-L-tartrate in the mid-infrared region in CCl_4 have been reported by Buffeteau et al.[21] before. As the alkyl group in dialkyl tartrates changes the spectra in the mid-infrared region, in the same solvent system they remain similar except for the region of 1500−1400 cm^{-1}, where the absorption bands of the alkyl group vibrations are expected to appear. In the C═O stretching region (1850−1600 cm^{-1}) one absorption band and bisignate VCD signals (negative at higher wavenumber and positive at lower wavenumber for D-enantiomer) are found in CCl_4 for the tartrates studied. In the 1500−900 cm^{-1} region three positive couplets (positive at lower frequency and negative at higher frequency for the D-enantiomer) are observed in the 1400−1240, 1240−1150, and 1150−1050 cm^{-1} regions in the VCD spectra in CCl_4. These VCD features are the same as those reported before except that the weak couplet in the 1240−1150 cm^{-1} region was not clearly seen[14,21] before for dimethyl-D-tartrate.

The experimental intrinsic rotation, $\{\alpha\}_D$, for dimethyl-D-tartrate is +43.0 in CCl_4. The experimental ORD of dimethyl-D-tartrate in CCl_4 (Figure 2) is monosignate and positive.

On the basis of previous VCD and NMR studies, the *trans*-COOR conformer (shown in Figure 3) was suggested to be the favored structure for dialkyl tartrates.[14,21] Rychlewska et al.[22] analyzed the conformations of isolated dimethyl-(*R*,*R*)-tartrate using ab initio calculations at the HF/6-31G* and MP2/6-31G* levels and proposed five lowest energy conformers. Among them, two *trans*-COOR conformers labeled by Rychlewska et al.[22] as T(ss) and T(as) are the lowest energy forms.[22] Recently

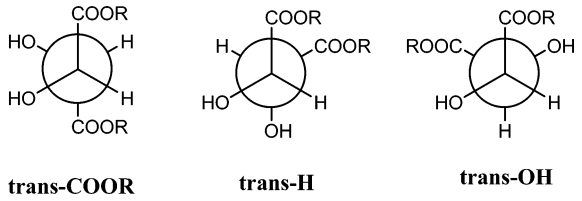

Figure 3. Three principle conformations of dialkyl-(*R,R*)-tartrate around the C*−C* bond.

Buffeteau et al.[21] reported predicted VA and VCD spectra using DFT theory for several conformers of dimethyl-(*R,R*)-tartrate in the isolated state and CCl_4. The B3LYP/6-31G* method was used for their calculations. It was found[21] that the experimental spectra in CCl_4 corresponded well with the predicted spectra for the T(s,s) conformer, which is same as the T(ss) conformer in the notation of Rychlewska et al.[22]

In the present study, DFT calculations were undertaken for isolated dimethyl-(*S,S*)-tartrate with a much larger aug-cc-pVDZ basis set than reported before. Twenty-two geometries for the isolated dimethyl-(*S,S*)-tartrate molecule were first optimized with the B3LYP/6-31G* method. These geometries and their electronic energies are given in Table S1 of the Supporting Information. The five lowest energy conformations (see Figure 4) were then reoptimized with a larger aug-cc-pVDZ basis set, and all of these conformations were found to have potential-energy minima (i.e., all vibrational frequencies are real). Four among these five conformers correspond to the lowest energy conformers identified by Rychlewska et al.[22] The most stable conformer noted in all previous studies corresponds to *trans*-$COOCH_3$-1 with two internal hydrogen bonds between the hydrogen atoms of OH groups and their nearest C═O groups. *trans*-$COOCH_3$-1 in the present notation corresponds to T(ss) in the notation of Rychlewska et al.[22] and T(s,s) in the notation of Buffeteau et al.[21] The second lowest energy conformer in the present study, *trans*-$COOCH_3$-2, has one internal hydrogen bond between the hydrogen atom of OH group and its nearest C═O; the hydrogen atom of the second OH group is approximately between the oxygen atom of first OH group and the nearest ester oxygen atom. The second lowest energy conformer identified by Rychlewska et al.[22] is T(as) with two internal hydrogen bonds: one between the hydrogen atom of one OH group and its nearest C═O and the other between the hydrogen atom of the other OH group and its nearest ester oxygen. We also considered the geometry of T(as), which in the present notation (Table S1 in Supporting Information) is *trans*-$COOCH_3$-9, but it was converted into the geometry of *trans*-$COOCH_3$-2 during geometry optimization. The *trans*-$COOCH_3$-2 conformer is also the second lowest energy conformer reported by Buffeteau et al.,[21] which in their notation is T(a,s).

The Gibbs energies, relative populations, and specific rotations predicted for the five lowest energy conformers of the isolated molecule using 6-31G* and aug-cc-pVDZ basis sets are listed in Table 1. *trans*-$COOCH_3$-1 is the predominant conformer for isolated dimethyl-(*S,S*)-tartrate. The absorption and VCD intensities were calculated for all five conformations at both the B3LYP/6-31G* and B3LYP/aug-cc-pVDZ levels. The absorption and VCD spectra at the B3LYP/aug-cc-pVDZ level for these five individual conformers of the isolated molecule and population-weighted sum of the absorption and

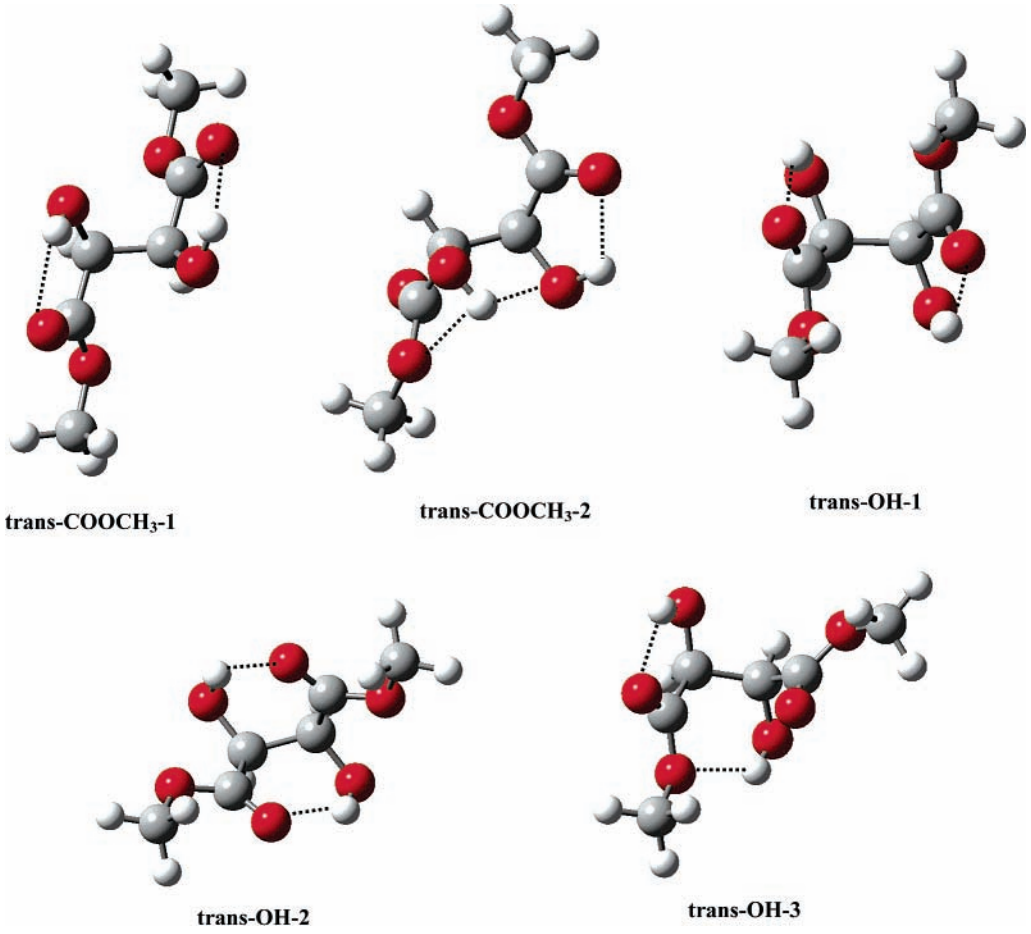

Figure 4. Five lowest energy conformers of isolated dimethyl-(*S,S*)-tartrate identified with B3LYP/6-31G* and B3LYP/aug-cc-pVDZ methods.

TABLE 1: B3LYP-Calculated Gibbs Energies, Populations, and Specific Rotations of the Five Lowest Energy Conformers of Isolated Dimethyl-(*S,S*)-tartrate

	trans-$COOCH_3$-1	*trans*-$COOCH_3$-2	*trans*-OH-1	*trans*-OH-2	*trans*-OH-3
		Gibbs energy (in Hartrees)			
6-31G*	−685.86466	−685.86270	−685.86158	−685.86160	−685.86066
aug-cc-pVDZ	−685.98342	−685.98113	−685.97953	−685.97774	−685.97799
		population(%)			
6-31G*	82.1	10.4	3.1	3.2	1.2
aug-cc-pVD Z	90.2	7.9	1.4	0.2	0.3
		specific rotation, $[\alpha]_D$			
6-31G*	65.2	−109.7	222.9	53.5	102.9
aug-cc-pVDZ	47.9	−120.8	209.9	42.2	103.4

VCD spectra of individual conformers are shown in Figure 5. The calculated frequencies (ν_i), dipole strengths (D_i), and rotational strengths (R_i) of five conformers of isolated dimethyl-(*S,S*)-tartrate at the B3LYP/aug-cc-pVDZ level are listed in Table 2. The predicted absorption and VCD spectra for the isolated dimethyl-(*S,S*)-tartrate (population-weighted sum of conformer spectra) at both the B3LYP/6-31G* and the B3LYP/aug-cc-pVDZ levels are compared with the experimental spectra of dimethyl-D-tartrate in CCl_4 in Figure 6. Experimental absorption and VCD band positions of dimethyl-D-tartrate in CCl_4 and their corresponding B3LYP-predicted values of isolated dimethyl-(*S,S*)-tartrate are listed in Table 3. The predicted absorption and VCD spectra at the B3LYP/6-31G* level are identical to those obtained at the B3LYP/aug-cc-pVDZ level except that frequencies of absorption and VCD bands in the predicted spectra at the B3LYP/aug-cc-pVDZ level are higher by about 10 cm^{-1} than those of the corresponding bands predicted at the B3LYP/6-31G* level. Overall, these predicted absorption and VCD spectra have good correspondence with the experimental spectra of dialkyl tartrates in CCl_4 in band positions and relative peak intensities. One notable disagreement in the VCD spectra is that a weak negative−positive doublet seen in the 1450−1350 cm^{-1} region in the predicted VCD spectrum does not have a corresponding couplet in the experimental spectrum.

The predicted specific rotations at 589 nm, obtained as the population-weighted sum of specific rotations of different conformers, are 50.4 at the 6-31G* basis and 38.8 at the aug-cc-pVDZ basis (Tables 1 and 4). These two predicted values, especially that predicted with the aug-cc-pVDZ basis set, are close to the experimentally observed intrinsic rotation of 43.0 in CCl_4. The predicted ORD for dimethyl-(*S,S*)-tartrate with the aug-cc-pVDZ basis set, as population-weighted values of the two lowest energy conformers of isolated dimethyl-(*S,S*)-tartrate (*trans*-$COOCH_3$-1 and *trans*-$COOCH_3$-2), compares well (Figure 2) with experimental ORD of dimethyl-D-tartrate in CCl_4.

Using the PCM model that was implemented in the Gaussian 03 program, optimization of the five lowest energy geometries of dimethyl tartrate obtained for the isolated molecule was also performed in CCl_4 solvent at the B3LYP/6-31G* level. The geometry of *trans*-OH-2 is found to be unstable in CCl_4. Buffeteau et al.[21] also reported that this conformer is not stable in the presence of CCl_4 solvent. The specific rotations and absorption and VCD intensities for the remaining four conformers were calculated at the B3LYP/6-31G* level with the PCM model.

The Gibbs energies, relative populations, and specific rotations predicted for the four conformers of the dimethyl tartrate in CCl_4 using the 6-31G* basis set are listed in Table 5. *trans*-$COOCH_3$-1 is still the predominant conformer for dimethyl-(*S,S*)-tartrate when CCl_4 solvent is represented by PCM.

From the calculated vibrational frequencies for dimethyl tartrate in CCl_4, all four conformers were found to have potential-energy minima. The population-weighted-predicted absorption and VCD spectra for dimethyl-(*S,S*)-tartrate in CCl_4 are shown in Figure 6. Experimental absorption and VCD band positions of dimethyl-D-tartrate in CCl_4 and their corresponding B3LYP-predicted values of dimethyl-(*S,S*)-tartrate in CCl_4 are listed in Table 3. The predicted absorption and VCD spectra of dimethyl-(*S,S*)-tartrate in CCl_4 do not differ significantly from those for the isolated molecule and correspond well with the experimental spectra of dialkyl tartrates in CCl_4. A weak negative−positive couplet in the 1450−1350 cm^{-1} region is

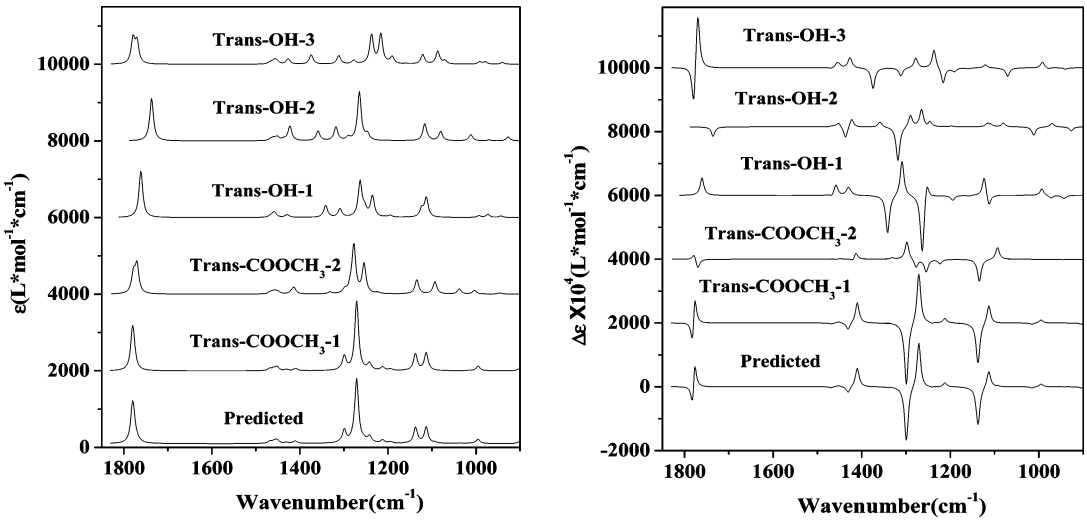

Figure 5. Simulated absorption (left) and VCD (right) spectra obtained for individual conformers of isolated dimethyl-(*S,S*)-tartrate at the B3LYP/aug-cc-pVDZ level. The population-weighted sum of conformer spectra is obtained with populations determined from the Gibbs energies (Table 1).

TABLE 2: Calculated Frequencies (ν_i), Dipole Strengths (D_i), and Rotational Strengths (R_i) of the Five Lowest Energy Conformers of Isolated Dimethyl-(*S,S*)-tartrate at the B3LYP/aug-cc-pVDZ Level[a]

trans-$COOCH_3$-1			*trans*-$COOCH_3$-2			*trans*-OH-1			*trans*-OH-2			*trans*-OH-3		
ν_i	D_i	R_i	ν_i	D_i	R_i	ν_i	D_i	R_i	ν_i	D_i	R_i	ν_i	D_i	R_i
1781	659.5	−332.6	1778	413.9	41.4	1762	167.4	−338.7	1738	24.2	137.7	1779	522.3	−292.8
1778	373.6	362.9	1770	596.9	−64.4	1761	835.7	450.3	1737	906.1	−195.8	1770	453.5	394.6
1431	31.7	−57.8	1413	165.6	56.4	1458	78.0	79.1	1437	41.5	−92.2	1374	259.4	−174.8
1410	60.6	167.3	1298	106.6	157.6	1431	52.0	53.9	1423	390.4	68.6	1312	248.3	−71.8
1299	403.1	−551.4	1278	1431.0	−75.0	1342	338.0	−326.7	1359	272.6	44.3	1278	107.3	89.6
1271	2063.6	456.2	1254	887.7	−114.1	1309	241.6	309.1	1318	392.6	−296.0	1238	467.6	−0.5
1242	208.4	−10.7	1223	39.7	−40.7	1263	1057.9	−540.5	1290	94.6	106.2	1237	414.6	170.9
1212	105.4	42.9	1135	476.8	−223.1	1253	237.3	170.5	1265	1456.5	156.2	1216	913.6	−148.8
1138	554.6	−411.7	1093	430.4	125.5	1235	642.9	1.0	1117	573.5	32.5	1190	219.8	−32.8
1113	607.9	192.2	1038	183.5	1.8	1123	266.7	198.3	1012	235.1	−93.6	1087	453.9	−5.1
995	176.9	35.3	1003	142.7	−3.3	1113	662.2	−124.8	927	162.0	−49.8	1071	114.2	−91.0

[a] Frequencies are in cm^{-1}, dipole strengths are in 10^{-40} esu^2 cm^2, and rotational strengths are in 10^{-44} esu^2 cm^2.

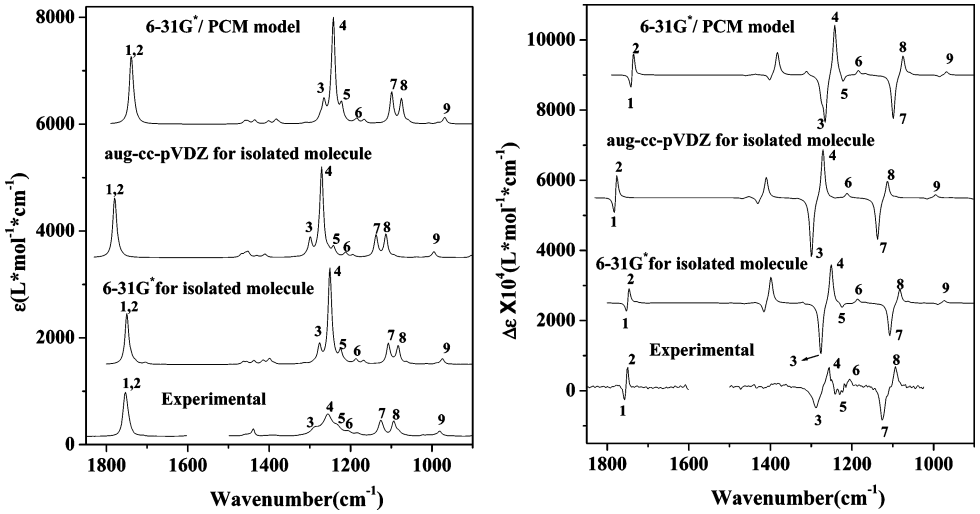

Figure 6. Comparison of the experimental absorption (left) and VCD (right) spectra of dimethyl-D-tartrate in CCl_4 with predicted absorption spectra for dimethyl-(*S,S*)-tartrate as isolated and solvated (CCl_4 represented by PCM).

TABLE 3: Experimental Absorption and VCD Band Positions[a] of Dimethyl-D-tartrate in CCl_4 and Their Correlation to B3LYP-Predicted Values of Dimethyl-(*S,S*)-tartrate in Vacuum and CCl_4

	experimental		predicted					
			6-31G* for isolated molecule[b]		aug-cc-pVDZ for isolated molecule		6-31G* with PCM model for CCl_4[b]	
no.	absorption	VCD	absorption	VCD	absorption	VCD	absorption	VCD
1,2	1752	1758 (−)[c]	1749	1750 (−)	1780	1781 (−)	1739	1740 (−)
		1748 (+)[c]		1748 (+)		1778 (+)		1737 (+)
3	1288	1288 (−)	1276	1276 (−)	1299	1299 (−)	1266	1266 (−)
4	1254	1254 (+)	1251	1251 (+)	1271	1271 (+)	1242	1242 (+)
5	1232	1232 (−)	1225	1225 (−)	1242		1222	1222 (−)
6	1206	1206 (+)	1200	1200 (+)	1212	1212 (+)	1185	1185 (+)
7	1125	1125 (−)	1107	1107 (−)	1138	1138 (−)	1099	1099 (−)
8	1096	1096 (+)	1083	1083 (+)	1113	1113 (+)	1075	1075 (+)
9	982	*d*	974	974 (+)	995	995 (+)	968	968 (+)

[a] Band positions are in cm^{-1}. [b] Predicted band positions at the B3LYP/6-31G* level were scaled with 0.96. [c] (+) refers to the positive sign of the VCD band, and (−) refers to the negative sign of the VCD band. [d] Corresponding VCD band is not found.

still present in the predicted VCD spectra, which does not have a counterpart in the experimental spectrum.

Only a small difference (less than 10%) is found for the specific rotation of each conformer in CCl_4 compared to that for isolated molecule. The population-weighted-predicted specific rotation is 53.2 at the 6-31G* basis. This predicted value in CCl_4 is close to the predicted value for the isolated molecule (see Table 4) and also to the experimental intrinsic rotation of dimethyl-D-tartrate in CCl_4.

(2) Dialkyl Tartrates in Dimethyl Sulfoxide. The vibrational absorption and VCD spectra of dialkyl tartrates in DMSO-d_6 solvent, in the 1850−1700 and 1600−1100 cm^{-1} regions, are shown in Figure 7. For a given tartrate, the absorption and VCD signals are affected significantly when the solvent is changed from CCl_4 to DMSO-d_6. In the C═O stretching region (1850−1600 cm^{-1}) two absorption bands and three VCD bands (negative−positive−negative triplet for D-enantiomers) are seen in DMSO-d_6 (while one absorption band and bisignate VCD signal, negative−positive for D-enantiomer, are found in CCl_4; Figure 1). In the ∼1200−1100 cm^{-1} region a weak negative VCD band at ∼1224 cm^{-1} and a negative couplet (positive at higher frequency and negative at lower frequency for D-enantiomers) are seen in DMSO-d_6. Another positive VCD signal and associated absorption band at ∼1090 cm^{-1}, also seen

TABLE 4: B3LYP-Predicted Specific Rotation, $[\alpha]_D$, of Dimethyl-(*S,S*)-tartrate, and Experimental Intrinsic Rotation, $\{\alpha\}_D$, of Dimethyl-D-tartrate

	predicted specific rotation $[\alpha]_D$		
	isolated molecule	in CCl_4	experimental intrinsic rotation $\{\alpha\}_D$
6-31G*	+50.4	+53.2	+43.0 ± 1.6
aug-cc-pVDZ	+38.8		

TABLE 5: B3LYP/6-31G*-Calculated Gibbs Energies, Populations, and Specific Rotations of Four Stable Conformers of Dimethyl-(*S,S*)-tartrate in CCl_4

	trans-$COOCH_3$-1	*trans*-$COOCH_3$-2	*trans*-OH-1	*trans*-OH-3
Gibbs energy (in Hartrees)	−685.87308	−685.87104	−685.86890	−685.86066
Population (%)	88.4	10.1	1.1	0.4
specific rotation, $[\alpha]_D$	70.0	−111.5	241.1	91.2

in DMSO,[14] are partially shown in Figure 7 as solvent interference occurs in this region.

The experimental intrinsic rotation, $\{\alpha\}_D$, of dimethyl-D-tartrate in DMSO solvent is −3.1 at 589 nm, which is very close to zero. For obtaining larger magnitudes optical rotation needs to be measured at shorter wavelengths. Therefore, the intrinsic rotation of dimethyl-D-tartrate was also measured at 365 nm in DMSO, where it is found to be +42.7. These two values at 589 and 365 nm indicate that specific rotation of dimethyl-D-tartrate changes from negative to positive as the wavelength decreases, suggesting bisignate ORD[12a,b] in DMSO. This observation is confirmed by measuring the ORD of dimethyl-D-tartrate at a concentration of 0.0064 M in DMSO (see Figure 8), which indicated that ORD is indeed bisignate with weak negative values at longer wavelengths and a change of sign near 546 nm.

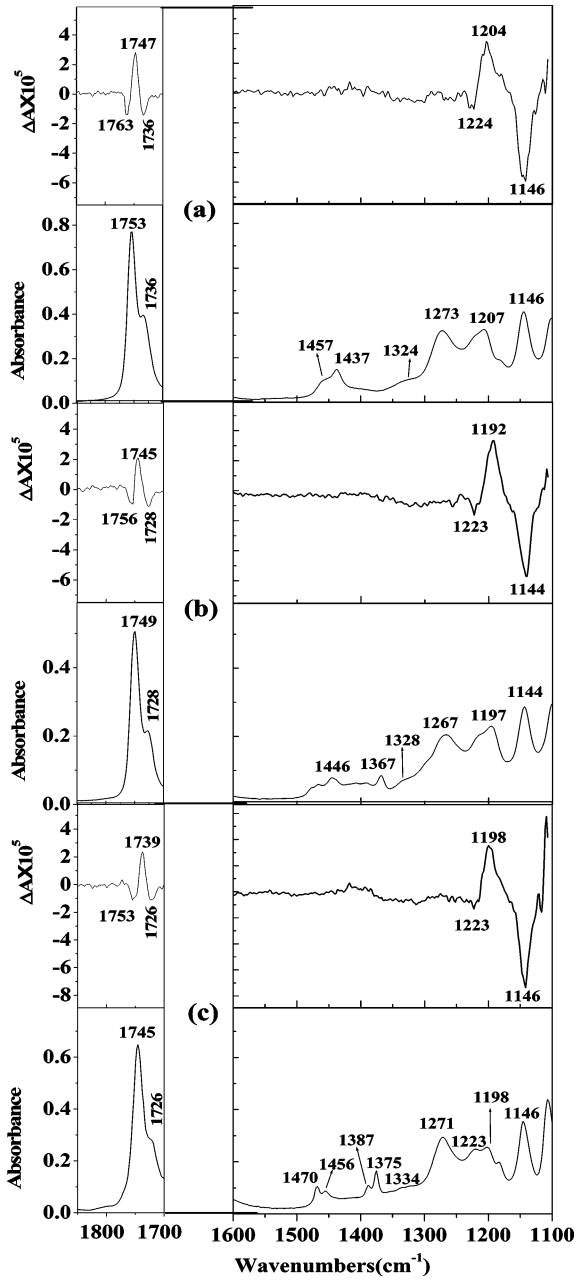

Figure 7. Vibrational absorption (bottom) and VCD (top) spectra in DMSO-d_6 solution: (a) dimethyl-D-tartrate (0.046 M), (b) diethyl-D-tartrate (0.040 M), and (c) diisopropyl-D-tartrate (0.035 M).

The DFT predictions of VCD (Figure 5) and optical rotation for isolated dimethyl tartrate molecule are not in agreement with the corresponding experimental data in DMSO (Figure 7). Thus, DMSO solvent influence needs to be incorporated into the calculations. For this purpose, attempts were made to use the PCM model, but geometry optimization in DMSO solvent with the PCM model could not be completed even after several weeks of computing time on a desktop computer. Therefore, clusters of dimethyl-(*S,S*)-tartrate and solvent molecules were considered to perform the calculation. Proniewicz et al.[23] reported a structural study of several hydroxamic acids in DMSO solutions based on the DFT calculations of NMR spectra. In their study they used clusters of hydroxamic acids with DMSO molecules, and the computed chemical shifts of these clusters were reported to be in good agreement with the experimental data.

Dimethyl-(*S,S*)-tartrate molecule has two −OH groups which are capable of forming hydrogen bonds with DMSO molecules. Therefore, a cluster with one dimethyl tartrate molecule interacting with two DMSO molecules is constructed. Two geometries for the *trans*-$COOCH_3$ cluster were considered first. Their structures are shown in Figure 9. In *trans*-$COOCH_3$-$(DMSO)_2$-0 cluster there are two intramolecular hydrogen bonds (between the OH group and C═O group, which are connected to the same

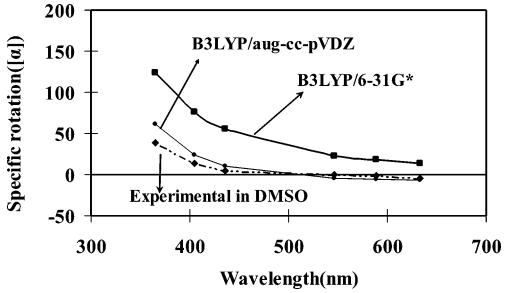

Figure 8. Comparison of experimental specific rotations of dimethyl-D-tartrate in DMSO and predicted specific rotations for dimethyl-(*S,S*)-tartrate in DMSO as a function of wavelength. The predicted specific rotations were obtained at the B3LYP/6-31G* and B3LYP/aug-cc-pVDZ levels as population-adjusted data from the two clusters, *trans*-$COOCH_3$-$(DMSO)_2$-1 and *trans*-H-$(DMSO)_2$-2.

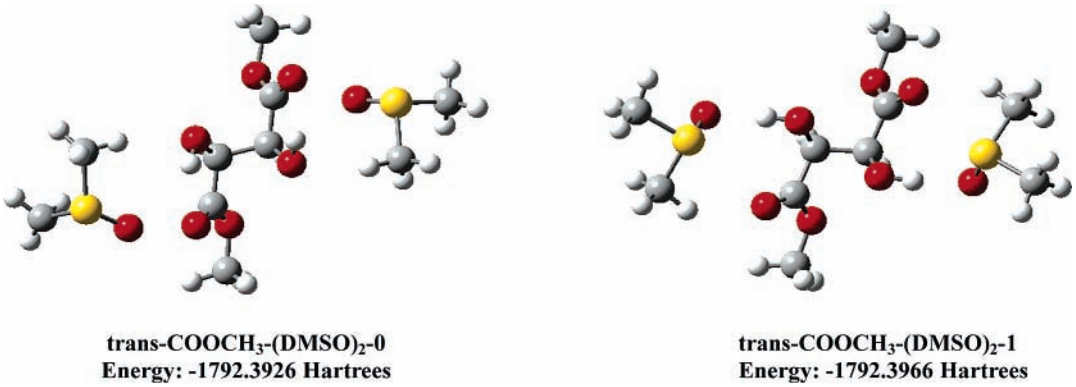

Figure 9. Structures and electronic energies obtained with the B3LYP/6-31G* method for *trans*-$COOCH_3$-$(DMSO)_2$-0 and *trans*-$COOCH_3$-$(DMSO)_2$-1 clusters.

chiral carbon) and solvent molecules remain as spectators; on the other hand, in *trans*-$COOCH_3$-$(DMSO)_2$-1 cluster the two hydrogen bonds are between the OH groups of dimethyl tartrate and S═O groups of solvent molecules. On the basis of their energies at optimized geometries with the B3LYP/6-31G* method (Figure 9), the *trans*-$COOCH_3$-$(DMSO)_2$-1 cluster is much more stable than the *trans*-$COOCH_3$-$(DMSO)_2$-0 cluster. Thus, it appears that in DMSO, dimethyl-(*S*,*S*)-tartrate prefers to form intermolecular hydrogen bonds with solvent molecules as opposed to forming intramolecular hydrogen bonds. Thus, the *trans*-$COOCH_3$, *trans*-OH, and *trans*-H clusters of dimethyl-(*S*,*S*)-tartrate with intermolecular hydrogen bonds to two DMSO molecules were investigated. Since OH groups of dimethyl tartrate are fixed in orientation to hydrogen bond to the S═O group of DMSO, only two conformers remain for each of the *trans*-$COOCH_3$, *trans*-OH, and *trans*-H clusters. The difference between these two conformers is in the orientation of the ester groups and C═O groups of dimethyl-(*S*,*S*)-tartrate (Figure 10). Thus, a total of six clusters was considered. The electronic energies and Gibbs energies were calculated for the six clusters of dimethyl-(*S*,*S*)-tartrate at the B3LYP/6-31G* level. The results are summarized in Table 6. Of these six clusters, *trans*-$COOCH_3$-$(DMSO)_2$-2 is found to have imaginary vibrational frequencies. The absorption, VCD, and optical rotation for the remaining five conformations with potential-energy minima were calculated at the B3LYP/6-31G* level. On the basis of Gibbs energies, *trans*-OH-$(DMSO)_2$-1 appeared to be the dominant conformer. However, the population-weighted-predicted absorption and VCD spectra (see Figure 11) and the predicted optical rotation (150.1 at 589 nm) are far from agreement with the corresponding experimental data. This disagreement indicated that the relative Gibbs energies of clusters may not have been predicted correctly.

Therefore, a different approach, based on the experimental intrinsic rotations and experimental VCD spectra, was used to suggest the possible dominant conformers and their populations. Specific rotations of the five clusters predicted at six wavelengths between 633 and 365 nm at the B3LYP/6-31G* level are given in Table 6. While *trans*-$COOCH_3$-$(DMSO)_2$-1 and *trans*-H-$(DMSO)_2$-2 clusters have small positive predicted specific rotations that are close to the experimental intrinsic rotations (at 589 and 365 nm), the remaining three conformations have very large predicted positive specific rotations. Thus, based on the specific rotation data alone, it appears that *trans*-$COOCH_3$-$(DMSO)_2$-1 and *trans*-H-$(DMSO)_2$-2 conformers are likely to be preferred in DMSO. This observation is further confirmed by reoptimizing the geometries of *trans*-$COOCH_3$ and *trans*-H clusters at B3LYP/aug-cc-pVDZ level and calculating the specific rotations of *trans*-$COOCH_3$ and *trans*-H clusters at the B3LYP/aug-cc-pVDZ level (see Table 6). When the predicted absorption spectra of these two clusters are combined, two absorption bands can be clearly seen in the C═O stretching region (Figure 12) which correspond well with the experimental absorption bands in this region for dialkyl tartrates in DMSO-d_6. When the predicted VCD spectra of these two clusters are combined, a negative−positive−negative triplet resulted in the C═O stretching region, which also has a good agreement with the experimental VCD bands for dialkyl-D-tartrates in this region. The observation that the intensities of two negative VCD bands of this triplet are nearly the same in the experimental VCD spectra of dialkyl tartrates is used to estimate the populations of these two clusters. It is found that with the populations of *trans*-$COOCH_3$-$(DMSO)_2$-1 and *trans*-H-$(DMSO)_2$-2 clusters as 62.5% and 37.5%, respectively, the two negative VCD bands in the predicted VCD spectrum of dimethyl-(*S*,*S*)-tartrate also have nearly the same peak intensities. These adjusted populations are therefore used to predict the absorption and VCD spectra of dimethyl-(*S*,*S*)-tartrate, and the resulting spectra are compared to the experimental spectra of dimethyl-D-tartrate in DMSO-d_6 (Figure 12). Experimental absorption and VCD band positions of dimethyl-D-tartrate in DMSO-d_6 and their corresponding values in the predicted spectra with adjusted populations are shown in Table 7. A good agreement is seen for the major absorption bands in the experimental and predicted spectra. Overall the bands in the experimental absorption spectrum are broader than those in the predicted spectrum and several small bands which appear in the 1300−1180 cm^{-1} region in the predicted spectrum have not been observed in the experimental spectrum. For the VCD spectra, there is a good agreement in the C═O stretching region (1850−1600 cm^{-1}) and also in the lower frequency region (1250−1100 cm^{-1}) for the VCD bands in predicted and experimental spectra. Two couplets with relatively low intensities are observed in the 1500−1400 cm^{-1} region in the predicted VCD spectrum, but these VCD bands are not present in the experimental spectrum. A similar discrepancy was also seen for the spectra in CCl_4 (Figure 6). The predicted specific rotations (with populations of *trans*-$COOCH_3$-$(DMSO)_2$-1 and *trans*-H-$(DMSO)_2$-2 clusters as 62.5% and 37.5%, respectively) are listed in Table 8 at both B3LYP/6-31G* and B3LYP/aug-cc-pVDZ levels. The B3LYP/6-31G*-predicted specific rotation (17.7) at 589 nm for dimethyl-(*S*,*S*)-tartrate differs in sign from that observed (−3.1) for dimethyl-D-tartrate. At 365 nm, however, the B3LYP/6-31G*-predicted specific rotation and experimental intrinsic rotation match in sign and magnitude and are not too far apart. The predicted specific rotations at B3LYP/aug-cc-pVDZ level for dimethyl-(*S*,*S*)-tartrate (−6.9 at 589 nm and 61.6 at 365 nm) match those observed for dimethyl-D-

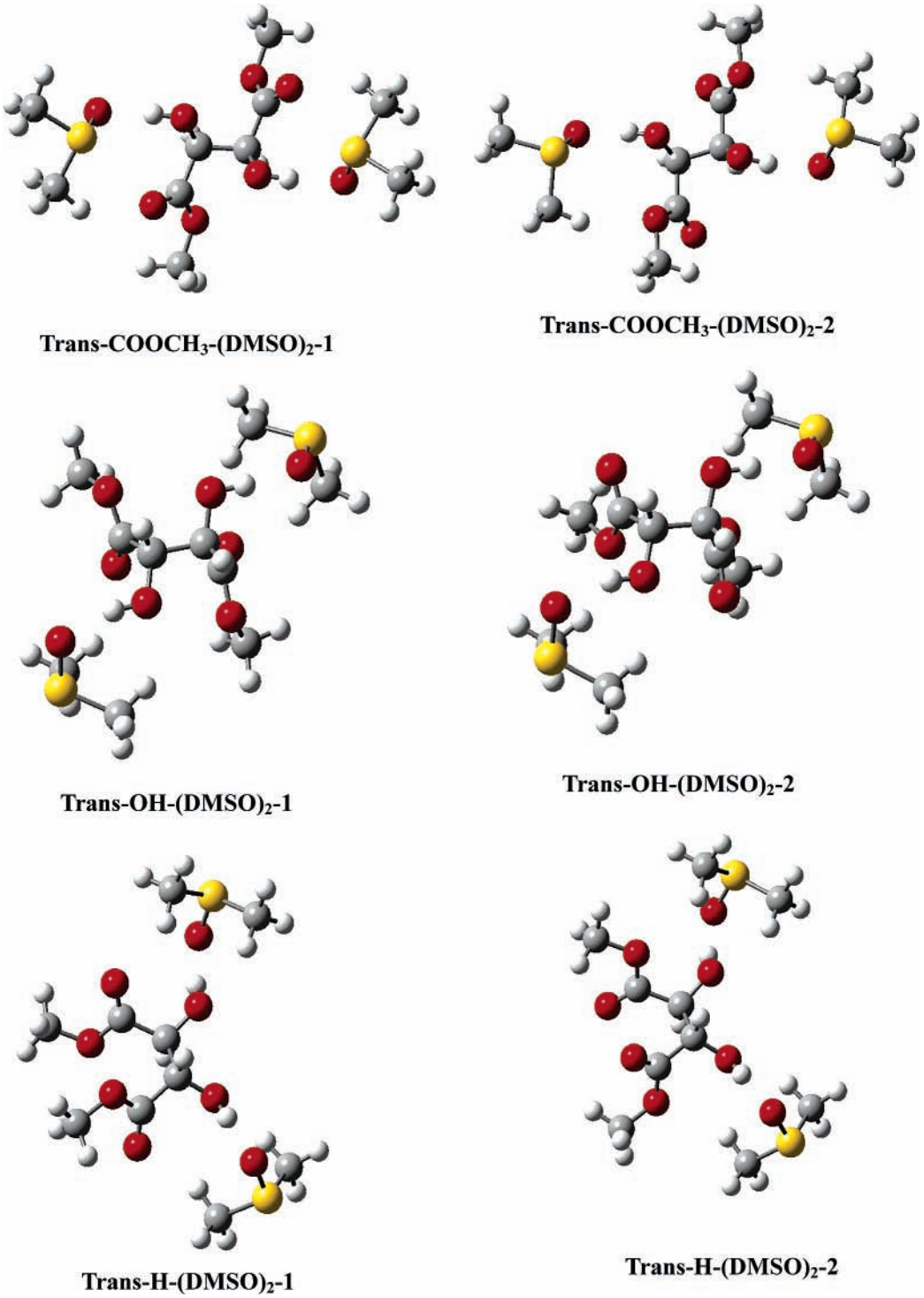

Figure 10. Structures of six clusters of dimethyl-(*S*,*S*)-tartrate with hydrogen bonds between OH groups of tartrate molecule and S═O groups of two DMSO molecules.

tartrate (−3.1 at 589 nm and 42.7 at 365 nm) at both 589 and 365 nm. The predicted ORD for dimethyl-(*S*,*S*)-tartrate in DMSO, at both B3lYP/6-31G* and B3LYP/aug-cc-pVDZ levels, obtained as population-weighted specific rotations of *trans*-$COOCH_3$-$(DMSO)_2$-1 and *trans*-H-$(DMSO)_2$-2 clusters, is compared with experimental ORD of dimethyl-D-tartrate in DMSO in Figure 8. The sign reversal seen in the experimental ORD data at about 546 nm is nicely reproduced in the B3LYP/aug-cc-pVDZ calculations but not in the B3LYP/6-31G* calculations. Even though the magnitudes of optical rotation at longer wavelengths are quite small, the magnitudes predicted at the B3LYP/aug-cc-pVDZ level are in very good agreement with those observed. It should be noted that for some molecules higher levels of theory were needed[24] for successfully predicting small magnitudes.

Thus, from VA, VCD, and ORD data it appears that a *trans*-$COOCH_3$ conformer, namely, *trans*-$COOCH_3$-$(DMSO)_2$-1, is still the dominant one in DMSO, but some amount of *trans*-H-$(DMSO)_2$-2 cluster is needed to explain the observed data in DMSO solvent.

(3) Dialkyl Tartrates in D_2O. Because of the interference from D_2O absorption, VCD spectra of dialkyl tartrates can only

TABLE 6: B3LYP-Calculated Gibbs Energies and Specific Rotations of Dimethyl-(*S,S*)-tartrate-$(DMSO)_2$ Clusters[a]

conformer	basis set	electronic energy (in Hartrees)	gibbs energy (in Hartrees)	percent population	specific rotation, [α] 633 nm	589 nm	546 nm	436 nm	405 nm	365 nm
trans-$COOCH_3$-$(DMSO)_2$-1	631G*	−1792.3966	−1792.1258	20.7	14.1	18.0	23.8	59.1	81.5	135.2
	aug-cc-pVDZ[b]	−1792.5950			−15.6	−16.3	−16.3	−2.6	13.0	59.8
trans-OH-$(DMSO)_2$-1	631G*	−1792.3999	−1792.1269	66.2	154.2	181.2	215.3	369.3	446.1	591.2
trans-OH-$(DMSO)_2$-2	631G*	−1792.3957	−1792.1243	4.2	126.2	148.8	177.5	309.8	377.4	508.0
trans-H-$(DMSO)_2$-1	631G*	−1792.3977	−1792.1250	8.8	194.1	229.0	273.5	479.7	586.0	793.4
	aug-cc-pVDZ[b]	−1792.5941			150.3	177.5	212.4	375.4	460.3	627.0
trans-H-$(DMSO)_2$-2	631G*	−1792.3935	−1792.1207	0.1	13.8	17.2	22.0	49.0	65.8	103.7
	aug-cc-pVDZ[b]	−1792.5901			8.62	10.7	13.6	30.3	40.7	64.5
experimental[c]					−4	−1(−3)	0	4	14	39(43)

[a] Specific rotations of *trans*-$COOCH_3$-$(DMSO)_2$-2 cluster (Figure 10) are not calculated as they has imaginary vibrational frequencies. [b] Obtained using aug-cc-pVDZ basis set at the corresponding optimized energy. [c] Experimental specific rotations at a concentration of 5 mg/mL; values in parentheses are intrinsic rotations.

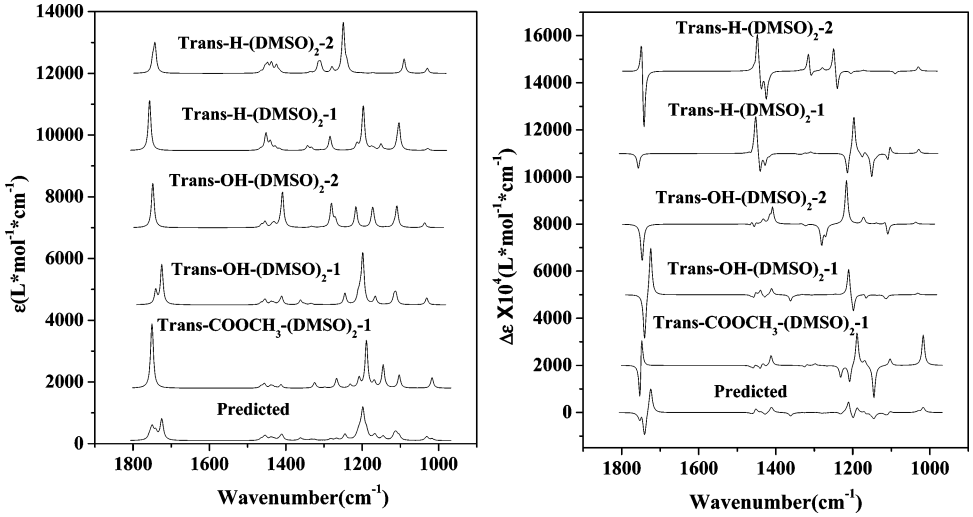

Figure 11. Simulated absorption (left) and VCD (right) spectra of dimethyl-(*S,S*)-tartrate clusters, and the population-weighted sum of cluster spectra at the B3LYP/6-31G* level.

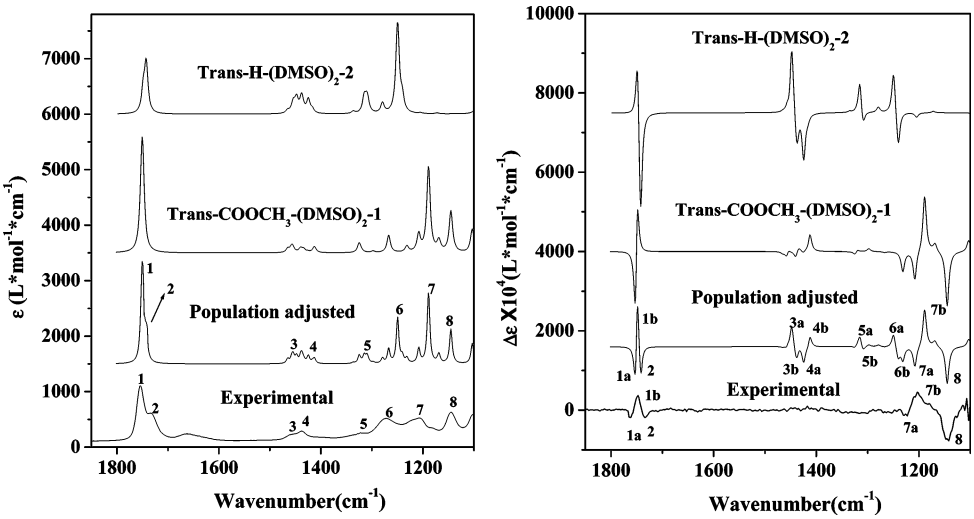

Figure 12. Comparison of the experimental absorption (left) and VCD (right) spectra of dimethyl-D-tartrate in DMSO-d_6 with the simulated spectra of *trans*-$COOCH_3$-$(DMSO)_2$-1 and *trans*-H-$(DMSO)_2$-2 clusters. The population-adjusted spectra of dimethyl-(*S,S*)-tartrate were obtained with populations of *trans*-$COOCH_3$-$(DMSO)_2$-1 and *trans*-H-$(DMSO)_2$-2 clusters as 62.5% and 37.5%, respectively.

be obtained in the region of 2000−1250 cm^{-1} in D_2O. The vibrational absorption and VCD spectra of dimethyl and diethyl tartrates, measured in D_2O solvent in the mid-infrared region, are shown in Figure 13. For a given tartrate, the absorption and VCD signals are affected significantly when the solvent is changed from CCl_4 to DMSO-d_6 to D_2O. In the C═O stretching region (1850−1600 cm^{-1}) one broader absorption band and no VCD signals are found in D_2O, while one absorption band and negative−positive VCD for the D-enantiomer are seen in CCl_4 (Figure 1), and two absorption bands and negative−positive−negative VCD triplet for the D-enantiomers are seen in DMSO-d_6 (Figure 7). The intrinsic rotation $\{\alpha\}_D$ for dimethyl-D-tartrate in H_2O solvent is −20.3. Thus, the intrinsic rotation of dimethyl-D-tartrate is also significantly affected when the solvent is changed from CCl_4 to DMSO to H_2O. The experimental ORD of dimethyl-D-tartrate in H_2O[12a] (not shown here) is monosignate

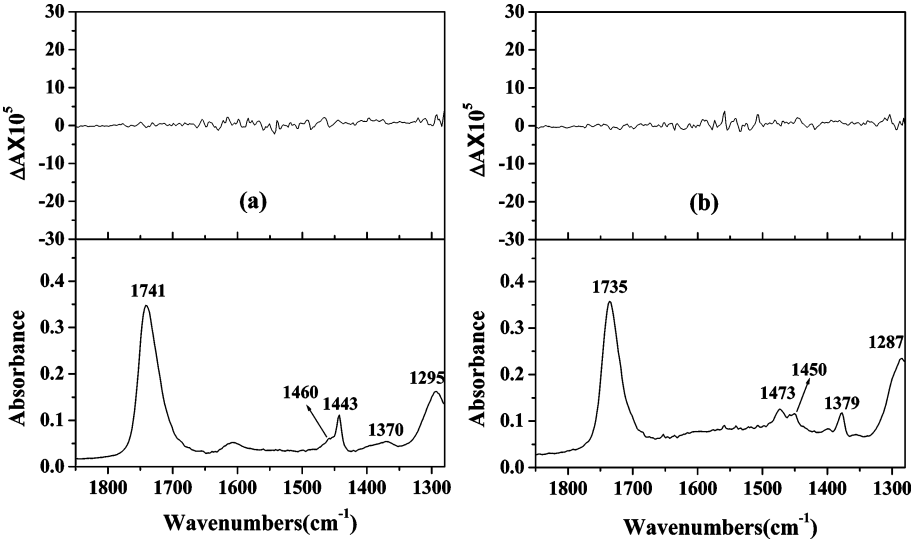

Figure 13. Vibrational absorption (bottom) and VCD (top) spectra in the C═O stretching region in D_2O solution of (a) dimethyl-D-tartrate (0.048 M) and (b) diethyl-D-tartrate (0.041 M).

TABLE 7: Experimental Absorption and VCD Band Positions[a] of Dimethyl-D-tartrate in DMSO-d_6 and Their Correlation to Predicted Values of Dimethyl-(*S,S*)-tartrate in DMSO

	experimental		predicted[b]	
no.	absorption	VCD	absorption	VCD
1	1753	1763 (−)[c]	1748	1750 (−)
		1747(+)[c]		1745 (+)
2	1736	1736(−)	1737	1737 (−)
3	1457	*d*	1445	1447 (+)
				1437 (−)
4	1437	*d*	1420	1422 (−)
				1410 (+)
5	1324	*d*	1311	1313 (+)
				1306 (−)
6	1273	*d*	1246	1248 (+)
				1234 (−)
7	1207	1224 (−)	1188	1207 (−)
		1204 (+)		1186 (+)
8	1146	1146 (−)	1142	1142 (−)

[a] Band positions are in cm^{-1}. [b] Predicted band positions at the B3LYP/6-31G* level from the population-adjusted spectra of *trans*-$COOCH_3$-$(DMSO)_2$-1 and *trans*-H-$(DMSO)_2$-2 clusters. [c] (+) refers to the positive sign of the VCD band, and (−) refers to the negative sign of the VCD band. [d] No corresponding VCD band is found.

TABLE 8: B3LYP-Predicted Specific Rotation [α] of Dimethyl-(*S,S*)-tartrate with Adjusted Populations,[a] and Experimental Intrinsic Rotation {α} of Dimethyl-D-tartrate in DMSO

	predicted [α]		
wavelength, nm	6-31G*	aug-cc-pVDZ	experimental {α}
589	17.7	−6.9	−3.1 ± 0.2
365	123.4	61.6	42.7 ± 0.4

[a] Populations of *trans*-$COOCH_3$-$(DMSO)_2$-1 and *trans*-H-$(DMSO)_2$-2 clusters used were 62.5% and 37.5%, respectively.

and negative, which is opposite to that in CCl_4 and different from that in DMSO.

Attempts to predict VA, VCD, and ORD for dimethyl-(*S,S*)-tartrate in H_2O posed several problems. The PCM model is not expected to capture all of the hydrogen-bonding effects in water completely. There are six oxygen atoms in dimethyl tartrate which can serve as hydrogen-bond acceptors and two hydroxyl groups which can serve as hydrogen-bond donors. Furthermore,

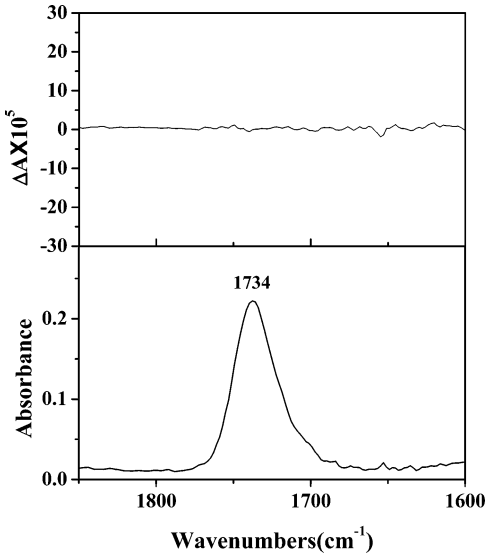

Figure 14. Vibrational absorption (bottom) and VCD (top) spectra in the C═O region in D_2O solution of diethyl-L-tartrate-α-CD complex (0.044 M).

H_2O molecules are both hydrogen-bond donors and acceptors (while DMSO molecules are just hydrogen-bond acceptors). Thus, it is difficult to determine the number of H_2O molecules needed to construct a realistic dimethyl tartrate cluster with water molecules. As a consequence, further investigations are needed to explain the observed VCD and ORD data in D_2O/H_2O solvent.

(4) Dialkyl Tartrate−Cyclodextrin Complexes. Dialkyl tartrate−cyclodextrin complexes were prepared using the co-precipitation method and characterized by ^1H NMR. From integration of the peaks in the NMR spectra, the complexation ratios for these complexes are confirmed to be 1:1.

The vibrational absorption and VCD spectra of dialkyl tartrate−cyclodextrin complexes were measured in D_2O and DMSO-d_6 solvents (see Figures 14 and 15). The absorption and VCD bands in the region below 1600 cm^{-1} originate from vibrational modes of both dialkyl tartrate and cyclodextrin molecules in the complex, while bands in the C═O stretching region (1850−1600 cm^{-1}) only come from carbonyl groups in dialkyl tartrates. A comparison between absorption and VCD

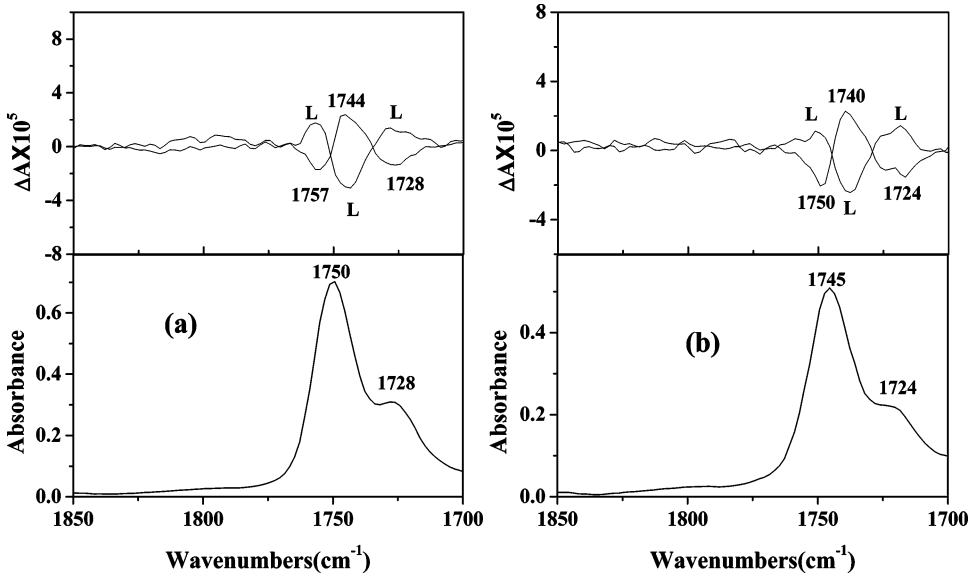

Figure 15. Vibrational absorption (bottom) and VCD (top) spectra in the C═O stretching region in DMSO-d_6 solution of (a) diethyl tartrate-β-CD complex (0.040 M) and (b) diisopropyl tartrate-β-CD complex (0.040 M). VCD spectra of both D- and L-tartrate complexes are shown; those labeled L are for L-tartrate complexes.

TABLE 9: Comparison of Intrinsic Rotations[a] of Dialkyl Tartate−Cyclodextrin Complexes with Those Estimated with the van't Hoff Principle of Optical Superposition

complex	experimental intrinsic rotation, $\{\alpha\}_D$	estimated intrinsic rotation, $\{\alpha\}_D$, of 1:1 complex[b]
diethyl-L-tartrate + α-CD	120.9 ± 0.7	129.5
diethyl-D-tartrate + β-CD	126.0 ± 0.9	130.6
diethyl-L-tartrate + β-CD	128.1 ± 1.2	138.9
diisopropyl-D-tartrate + β -CD	125.5 ± 0.9	126.7
diisopropyl-L-tartrate + β-CD	132.4 ± 1.2	136.9

[a] Intrinsic rotations of α-CD, β-CD, diethyl-D-tartrate, diethyl-L-tartrate, diisopropyl-D-tartrate, and diisopropyl-L-tartrate in water are, respectively, 151.0 ± 0.5, 159.1 ± 0.4, −26.0 ± 0.2, +28.0 ± 0.2, −30.0 ± 0.3, and 29.3 ± 0.4. [b] Estimated with the van't Hoff principle of optical superposition using eq 1.

bands in the C═O region of dialkyl tartrates with those of their corresponding complexes can reveal the effects of complexation with cyclodextrin on dialkyl tartrates. The absorption and VCD signals in the C═O region for these complexes are identical to those seen in the spectra of dialkyl tatrates: in D_2O, one broader absorption band and no VCD signals are found (Figures 13 and 14); in DMSO-d_6 (Figures 7 and 15), there are two absorption bands and three VCD bands (negative−positive−negative triplet for D-tartrate complexes). The frequencies of these bands for complexes in the C═O region are almost the same as those for dialkyl tartrates.

The intrinsic rotations of dialkyl tartrate−cyclodextrin complexes were measured in H_2O. They are compared with those estimated using van't Hoff's principle of optical superposition[25] for 1:1 complexes of dialkyl tartrate and cyclodextrin in Table 9. The intrinsic rotations estimated with van't Hoff's principle of optical superposition are given by eq 1[26]

$$\{\alpha\}_{\text{complex}} = \{\alpha\}_{\text{guest}} \times \frac{M_{\text{guest}}}{M_{\text{complex}}} + \{\alpha\}_{host} \times \frac{M_{\text{host}}}{M_{\text{complex}}} \qquad (1)$$

where $\{\alpha\}$ is intrinsic rotaton, M is molar mass, and the subscript "guest" represents dialkyl tartrate molecule and "host" represents cyclodextrin molecule. The observed intrinsic rotations of dialkyl tartrate−cyclodextrin complexes are close to the estimated values with differences between them being less than 10% in all cases.

From the comparison of VA and VCD spectra of dialkyl tartrate−cyclodextrin complexes with those of dialkyl tartrates in the C═O stretching region and comparison of intrinsic rotations of dialkyl tartrate−cyclodextrin complexes with those of estimated rotations, it becomes apparent that in the solution of DMSO and H_2O the interaction between dialkyl tartrates and cyclodextrin must be weak or the crystalline dialkyl tartrate−cyclodextrin complexes may have dissociated upon dissolution in DMSO or H_2O. In order to determine which one of these possibilities may have actually occurred, one needs to know the binding constants for dialkyl tartrate−cyclodextrin complexes in solution. The binding constants of dialkyl tartrate−cyclodextrin complexes are not available in the literature, so we measured these binding constants for the first time.

First, we attempted the quantitative NMR method[27] to measure the binding constants of dialkyl tartrate−cyclodextrin complexes in DMSO and H_2O, but these data indicated large errors in the resulting binding constants. Isothermal titration calorimetry (ITC) is a thermodynamic technique that allows the study of the interactions of two species.[17] When these two species interact, heat is either generated or absorbed. By measuring these interaction heats, binding constants (K), reaction stoichiometry (n), and thermodynamic parameters including enthalpy (ΔH) and entropy (ΔS) can be accurately determined. ITC is a direct, accurate, and highly sensitive method to measure binding constants and other thermodynamic parameters. ITC has found widespread applicability in the study of biological systems[28] involving protein−ligand, protein−nucleic acid, and

TABLE 10: Binding Constants of Diethyl-L-tartrate and Cyclodextrin in Solutions

host	solvent	binding constant (M^{-1})
α-CD	H_2O	62.2 ± 1.4
α-CD	DMSO	30.2 ± 6.1
β-CD	H_2O	39.0 ± 1.7
β-CD	DMSO	23.6 ± 6.9

protein−protein interactions and also in supramolecular chemistry, most notably for cyclodextrins (CDs)[29] and crown ethers.[30]

Calorimetric titrations were made for α-CD and *β*-CD with diethyl-L-tartrate in both H_2O and DMSO. The calorimetric titration plots are given in the Supporting Information. The binding constants of diethyl-L-tartrate complexes with α-CD and *β*-CD in H_2O and DMSO solvents are listed in Table 10. The binding constants between diethyl-L-tartrate and cyclodextrin (α-CD or *β*-CD) in DMSO are smaller than their corresponding binding constants in H_2O. Generally, these binding constants are very small ($<100\ M^{-1}$) in both H_2O and DMSO. From these data it can be concluded that dialkyl tartrate−cyclodextrin complexes do exist in solutions of H_2O and DMSO, but the interaction between diethyl-L-tartrate and cyclodextrin (α-CD or *β*-CD) is very weak. This observation can explain why the absorption, VCD, and optical rotation properties of dialkyl tartrates are not affected significantly upon complexation with cyclodextrin in solution.

Conclusions

The VA and VCD spectra in the mid-infrared region, intrinsic rotations, and ORD spectra of dialkyl tartrates are found to be solvent dependent. The DFT calculations for dimethyl-(*S*,*S*)-tartrate, a representative compound among these tartrates, were performed in the isolated state and in two different solvents. The *trans*-COOR conformer with hydrogen bonding between the OH and C═O groups attached to the same chiral carbon is dominant for isolated dimethyl-(*S*,*S*)-tartrate and also for dimethyl-(*S*,*S*)-tartrate in CCl_4. The population-weighted VA and VCD spectra, specific rotations, and ORD for isolated dimethyl-(*S*,*S*)-tartrate and for dimethyl-(*S*,*S*)-tartrate in CCl_4 correspond well with the experimental data in CCl_4. In DMSO, dimethyl-(*S*,*S*)-tartrate molecules favor formation of intermolecular hydrogen-bonded clusters with DMSO solvent molecules. On the basis of the experimental and predicted results in DMSO, a *trans*-COOR cluster appears to be the dominant conformer along with some amount of *trans*-H cluster. When the predicted VA and VCD spectra, specific rotations, and ORD of these two clusters are combined, the resulting data are in reasonable agreement with the experimental data of dimethyl-D-tartrate in DMSO solvent. For dialkyl tartrate−cyclodextrin complexes, cyclodextrin does not influence the VA, VCD, and intrinsic rotation properties of dialkyl tartrates significantly upon complexation. Binding constants, determined using isothermal titration calorimetry, for cyclodextrin−dialkyl tartrate complexes have small magnitudes, which confirmed that the interaction between cyclodextrin and dialkyl tartrates is indeed very weak.

Acknowledgment. We thank Dr. Laura Mizoue of the Vanderbilt University Center for Structural Biology for use of the isothermal titration calorimeter.

Supporting Information Available: NMR data on cyclodextrin−tartrate complexes, table with description and energies of 22 conformers investigated at the B3LYP/6-31G* level, optical rotation plots as a function of concentration, and isothermal calorimetric titration plots. This material is available free of charge via the Internet at http://pubs.acs.org.

References and Notes

(1) (a) Gawronski, J.; Dlugokinska, A.; Grajewski, J.; Plutecka, A.; Rychlewska, U. *Chirality* **2005**, *17*, 388−395. (b) Gawronski, J.; Skowronek, P. *Curr. Org. Chem.* **2004**, *8*, 65−82. (c) Gawronski, J.; Gawronska, K.; Skowronek, P.; Rychlewska, U.; Warzajtis, B.; Rychlewski, J.; Hoffmann, M.; Szarecka, A. *Tetrahedron* **1997**, *53*, 6113−6144. (d) Gawronski, J.; Gawronska, K.; Rychlewska, U. *Tetrahedron Lett.* **1989**, *30*, 6071−6074.

(2) (a) Johnson, R. A.; Sharpless, K. B. In *Catalytic Asymmetric Synthesis*, 2nd ed.; Ojima, I., Ed.; Wiley-VCH: New York, 2000; Chapter 6A, p 231. (b) Seebach, D.; Beck, A. K.; Heckel, A. *Angew. Chem., Int. Ed.* **2001**, *40*, 92−138.

(3) (a) Galwas, P. A. Ph.D. Thesis, Cambridge University, 1983. (b) Buckingham, A. D.; Fowler, P. W.; Galwas, P. A. Chem. *Phys.* **1987**, *112*, 1−14. (c) Stephens, P. J. *J. Phys. Chem.* **1985**, *89*, 748−752.

(4) Koch, W.; Holthausen, M. C. *A chemist's guide to density functional theory*, 2nd ed.; Wiley-VCH: New York, 2001.

(5) (a) *Gaussian 98/03*; Gaussian Inc.: Pittsburgh, PA; www.gaussian.com. (b) *Dalton, a molecular electronic structure program*; University of Oslo: Oslo, 2001; www.kjemi.uio.no/software/dalton/.

(6) (a) Polavarapu, P. L.; He, J. *Anal. Chem.* **2004**, *76*, 61A−67A. (b) Freedman, T. B.; Cao, X.; Dukor, R. K.; Nafie, L. A. *Chirality* **2003**, *15*, 743−758. (c) Stephens, P. J.; Devlin, F. J. *Chirality* **2000**, *12*, 172−179.

(7) (a) Bose, P. K.; Polavarapu, P. L. *Carbonhydr. Res.* **2000**, *323*, 63−72. (b) Setnicka, V.; Urbanova, M.; Kral, V.; Volka, K. *Spectrochim. Acta A* **2002**, *58*, 2983−2989.

(8) Polavarapu, P. L. *Mol. Phys.* **1997**, *91*, 551−554.

(9) (a) Carwford, T. D. *Theor. Chem. Acc.* **2006**, *115*, 227−245. (b) Polavarapu, P. L. *Chirality* **2002**, *14*, 768−781.

(10) (a) Muller, T.; Wiberg, K. B.; Vaccaro, P. H. *J. Phys. Chem. A* **2000**, *104*, 5959−5968. (b) Muller, T.; Wiberg, K. B.; Vaccaro, P. H. *Rev. Sci. Instrum.* **2002**, *73*, 1340−1342. (c) Muller, T.; Wiberg, K. B.; Vaccaro, P. H.; Cheeseman, J. R.; Frisch, M. J. *J. Opt. Soc. Am. B: Opt. Phys.* **2002**, *19*, 125−141. (d) Wilson, S. M.; Wiberg, K. B.; Cheeseman, J. R.; Frisch, M. J.; Vaccaro, P. H. *J. Phys. Chem. A* **2005**, *109*, 11752−11764.

(11) Polavarapu, P. L.; Petrovic, A.; Wang, F. *Chirality* **2003**, *15*, S143−S149.

(12) (a) Polavarapu, P. L.; Petrovic, A. G.; Zhang, P. *Chirality* **2006**, *18*, 723−732. (b) Polavarapu, P. L. *Chirality* **2006**, *18*, 348−356. (c) Giorgio, E.; Viglione, R. G.; Zanasi, R.; Rosini, C. *J. Am. Chem. Soc.* **2004**, *126*, 12968−12976. (d) Autschbach, J.; Jensen, L.; Schatz, G. C.; Electra Tse, Y. C.; Krykunov, M. *J. Phys. Chem. A* **2006**, *110*, 2461−2473.

(13) Su, C. N.; Keiderling, T. A. *J. Am. Chem. Soc.* **1980**, *102*, 511−515.

(14) Polavarapu, P. L.; Ewig, C. S.; Chandramouly, T. *J. Am. Chem. Soc.* 1**987**, *109*, 7382−7386.

(15) Shanmugam, G.; Polavarapu, P. L. *J. Am. Chem. Soc* **2004**, *126*, 10292−10295.

(16) Hedges, A. R. *Chem. Rev.* **1998**, *98*, 2035−2044.

(17) Freire, E.; Mayorga, O. L.; Straume, M. *Anal. Chem.* **1990**, *62*, 950A-959A.

(18) (a) Becke, A. D. *J. Chem. Phys.* **1993**, *98*, 5648−5652. (b) Lee, C.; Yang, W.; Parr, R. G. *Phys. Rev. B* **1988**, *37*, 785−789. (c) Vosko, S. H.; Wilk, L.; Nusair, M. *Can J Phys.* **1980**, *58*, 1200.

(19) (a) Hariharan, P. C.; Pople, J. A. *Chem. Phys. Lett.* **1972**, *16*, 217−219. (b) Dunning, T. H., Jr. *J. Chem. Phys.* **1989**, *90*, 1007−1023.

(20) Wong, M. W. *Chem. Phys. Lett.* **1996**, *256*, 391−399.

(21) Buffeteau, T.; Ducasse, L.; Brizard, A.; Huc, I.; Oda, R. *J. Phys. Chem. A* **2004**, *108*, 4080−4086.

(22) Rychlewska, U.; Warzajtis, B.; Hoffmann, M.; Rychlewski, J. *Molecules* **1997**, *2*, 106−113.

(23) (a) Kaczor, A.; Proniewicz, L. M. *J. Mol. Struct.: Theochem* **2003**, *640*, 133−41. (b) Kaczor, A.; Proniewicz, L. M. *J. Mol. Struct.* **2004**, *704*, 189−96.

(24) Kongsted, J.; Pedersen, T. B.; Jensen, L.; Hansen, A. E.; Mikkelsen, K. V. *J. Am. Chem. Soc.* **2006**, *128*, 976−982.

(25) (a) van't Hoff, G. H. *Bull. Soc. Chim. Fr.* **1875**, *23*, 295−301. (b) van't Hoff, G. H. *Die lagerung der Atome in Raum*; Branschweig: Vieweg, 1908.

(26) The van't Hoff principle of optical superposition can be interpreted to suggest that, at a given wavelength λ, the intrinsic molar rotation $\{\phi\}_\lambda$ of a host−guest complex is equal to the sum of molar rotations of host and guest that constitute the complex. That is, $\{\phi\}_\lambda = \{\phi_g\}_\lambda + \{\phi_h\}_\lambda$, where subscripts g and h represent guest and host, respectively. Thus, eq 1 can be derived using the definition for intrinsic molar rotation, $\{\phi_i\}_\lambda = \{\alpha_i\}_\lambda \times M_i/100$, where $\{\alpha_i\}_\lambda$ is the intrinsic rotation of i at wavelength λ and M_i is the molar mass of i.

(27) Andini, S.; Castronuovo, G.; Elia, V.; Gallotta, E. *Carbonhydr. Res.* **1991**, *217*, 87−97.

(28) (a) Cooper, A. *Curr. Opin. Chem. Biol*. **1999**, *3*, 557−563. (b) Haq, I. Ladbury, J. E. *J. Mol. Recognit.* **2000**, *13*, 188−197. (c) Leavitt, S.; Freire, E. *Curr. Opin. Struct. Biol*. **2001**, *11*, 560−566. (d) Weber, P. C.; Salemme, F. R. *Curr. Opin. Struct. Biol*. **2003**, *13*, 115−121.

(29) Rekharsky, M. V.; Inoue, Y. *Chem. Rev.* **1998**, *98*, 1875−1917.

(30) (a) Izatt, R. M.; Terry, R. E.; Haymore, B. L.; Hansen, L. D.; Dalley, N. K.; Avondet, A. G.; Christensen, J. J. *J. Am. Chem. Soc.* **1976**, *98*, 7620−7630. (b) Ozutsumi, K.; Ishiguro, S.-I. *Bull. Chem. Soc. Jpn.* **1992**, *65*, 1173−1175.